1 Flow and Correlations

1.1 Introduction

High energy nuclear collisions at RHIC and the LHC produce a relativistic fluid composed of QCD matter, i. e. quarks and gluons. It is particularly interesting to study the macroscopic properties of this fluid because - at least conceptually - they are fully fixed by the microscopic properties of a renormalizable, fundamental quantum field theory, namely QCD. One can study here experimentally, as well as theoretically, how macroscopic material properties result from microscopic field theoretic processes. Many theoretical methods ranging from perturbative to non-perturbative techniques are being developed to understand this in detail and one can expect that the insights gained here will be valuable for many related problems in fields ranging from condensed matter theory to cosmology in the future.

One must say that currently the field is still largely driven by experimental progress. Theoretically, the connection between microscopic QCD physics and the macroscopic properties of the quark-gluon plasma are being understood step by step but a satisfactory understanding is still missing.

Many different fronts of research are being explored at the moment. This ranges from conceptual questions on how to consistently formulate relativistic fluid dynamics or how to solve quantum field theory in non-equilibrium situations to very concrete practical questions about the thermodynamic and transport properties (such as viscosities or conductivities) of the quark-gluon plasma. Besides the role of strong interactions, also electromagnetic interactions and in particular the role of magnetic fields and the production of photons and dileptons is being explored. Other fronts of research concern the role of quantum anomalies, chirality and vorticity or the dependence of collective behavior on system size (nucleus-nucleus versus proton-nucleus and proton-proton collisions), on centrality and collision energy, the initial state directly after the collision, or various types of fluctuations. We will discuss these issues in more detail in the following subsections.

- General introduction
- Why is it interesting to study the fluid dynamics of the QGP
- What has been learnt so far at LHC
- What questions remain

2 Macroscopic properties

– short summary of traditional flow measurements at LHC
– Flow fluctuations, multi-particle clumulants, EbE vn
– how present LHC measurements constrain shear and bulk viscosity
– can we constrain temperature dependence of viscosity
– what we have learnt about EOS

2.1 QCD Equation of State

The QCD equation of state, accessible in high-energy collisions (and in the region around mid-rapidity) is that at vanishing baryon chemical potential, and it has been established for some time that it features a crossover transition to a chirally symmetric quark gluon plasma [1]. Most recent lattice calculations [2] have determined the cross-over temperature to be $T_c \simeq 156.5 \pm 1.5\,\mathrm{MeV}$. Recent efforts are also exploring the equation of state at finite μ_B, which at LHC would have relevance mainly at very forward rapidities. Here, because of the sign problem, methods like Taylor expansion [3–6] or imaginary chemical potentials [7–11] have to be employed.

To employ lattice QCD based equations of state in hydrodynamic caluclations, they need to be matched to a hadron resonance gas model at low temperatures, to cover the entire temperature range from zero to the maximally reached teperature. Various equations of state [12–14], using different lattice data and different matching conditions have been used in simulations. A comparison of some of them can be found in [15]. In this work the sensitivity of observables to the choice of equation of state was studied. While the mean transverse momentum varied by approximately 3% when using different equations of state, v_2 and v_3 changed by 8% and 15%, respectively. Because different lattice data was used, and matching to the hadron resonance gas was performed at a higher temperature, the s95p-v1 lattice parameterization has a smaller speed of sound in an extended temperature regime, compared to the other equations of state. This leads to a reduced amount of flow.

Such differences will affect the precise extraction of transport coefficients, such as η/s and ζ/s. Fortunately, the newer lattice QCD equations of state from the hotQCD collaboration [14] and the Wuppertal-Budapest collaboration [13] lead to differences only on the percent level for the studied observables.

Currently, the experimental data can not easily teach us directly about the equation of state, because of the uncertainty in the transport coefficients. One possibility would be to extend state of the art Bayesian techniques [16] to include free parameters describing the equation of state and fit them along with other free parameters such as shear and bulk viscosities.

2.2 Shear viscosity of hot nuclear matter

Ideal fluid dynamics has been very succesful in describing a variety of bulk observables in heavy ion collisions [17–19], indicating early on that the shear and bulk viscosities of the produced matter cannot be large. Calculations in the strong coupling limit using gauge gravity duality have found a value of $\eta/s = 1/4\pi$ for an $N = 4$ super Yang-Mills quantum system. This value was significantly smaller than the η/s obtained in perturbative QCD calculations, which were, however, plagued by significant errors, mainly resulting from uncertainties in the relevant scales [20]. Recently, such perturbative calculations have been extended to include next-to-leading order corrections and aa significant reduction compared to the leading order result was found [21]: At temperatures of the order of the QCD transition the NLO η/s is smaller by a factor of 5 compared to the LO result, and reaches values of approximately $2/4\pi$.

Extractions of transport coefficients from lattice QCD calculations [22–24] are extraordinarily hard, because the spectral function for use in the Kubo formula follows from a difficult inversion of an

integral transform of a correlator of the energy momentum tensor. Most recent calcaultations for a pure gluon plasma find $\eta/s = 0.17 \pm 0.02$ at $T = 1.5\,T_c$.

Apart from above direct calculations of the shear viscosity to entropy density ratio, by means of hydrodynamic simulations its value can be extracted by comparison to experimental data [25, 26]. This method suffers mainly from uncertainties in the initial state (see Section 3). The latest constraints come from simulations using the IP-Glasma initial state [27, 28], the EKRT model [29] and Bayesian analyses employing the Trento initial state model [16]. IP-Glasma + hydrodynamic simulations including bulk and shear viscosity find for the shear viscosity an effective constant value of $\eta/s = 0.095$ at the $\sqrt{s} = 2.76\,\mathrm{TeV}$ LHC energy and $\eta/s = 0.06$ at the top RHIC energy. EKRT simulations find good agreement with LHC data using a constant value of $\eta/s = 0.2$ and also certain temperature dependent η/s values. Finally, the latest Bayesian analyses of $\sqrt{s} = 5\,\mathrm{TeV}$ Pb+Pb collisions at the LHC using the Trento initial state determined an approximately linearly rising η/s with temperature, with $(\eta/s)(T = 150\,\mathrm{MeV}) \approx 0.09$ and $(\eta/s)(T = 300\,\mathrm{MeV}) \approx 0.16$.

The method of extracting η/s using hydrodynamic simulations and comparison to experimental data thus leaves us with an uncertainty of approximately a factor of 3 at this point. Comparison to more observables that would allow to independently better constrain features of the initial state and medium properties will hopefully reduce this uncertainty in the future.

2.3 Bulk viscosity of hot nuclear matter

There are several theoretical indications that bulk viscosity could play an important role in the transition region of QCD (see [30] and references therein). Similar to the case of shear viscosity, bulk viscosity over entropy density ratios have been calculated using holography in the strong coupling regime using extensions to non-conformal theories [31, 32]. The temperature dependent ζ/s features a peak of value 0.05 around a temperature of $\sim 160\,\mathrm{MeV}$. Perturbative calculations have shown that the simple estimate $\zeta \approx 15\eta(1/3 - c_s^2)^2$ [33] is parametrically correct for QCD [34], where $(1/3 - c_s^2)$ is the deviation from conformal symmetry. Lattice calculations using the Kubo formula extract large values of ζ/s around T_c [35, 36], with large uncertainties for the value at T_c, which is of order 1 [37], and exhibit a fast drop with increasing T.

Parametrizations of the bulk viscosity over entropy density's temperature dependence were performed in [38] with input from [35] for the QGP phase and [39] for the hadronic phase. This parametrization features a peak of ζ/s around $T \approx 180\,\mathrm{MeV}$, reaching approximately a value of 0.3. It has been used in various hydrodynamic simulations employing the IP-Glasma initial state and led to good agreement of the calculated mean transverse momentum with experimental data. Calculations using other initial states have reported the need for smaller bulk viscosity over entropy density values. For example in a recent Bayesian analyss using the Trento initial state model, ζ/s peaks at a value about 10 times smaller. In [40] it was discussed how the compact size and initial flow present in the IP-Glasma initial state contribute to the need for a larger bulk viscosity compared to other initial state models.

Viscous corrections to the distribution function at freeze-out affect the low p_T part of the spectrum more for bulk viscosity than for the shear part [41, 42]. Consequently, the uncertainties resulting from bulk viscous corrections are typically larger than for shear when studying p_T integrated observables.

2.4 Heat conductivity

Bulk diffusion, can we constrain it?

2.5 Electric conductivity

can we constrain it? Relevance for magnetic fields, Chiral magnetic effect

2.6 Second order transport properties

A peculiar feature of relativistic fluid dynamics is that it is not always causal. More specifically, this problem arises when one goes beyond the ideal fluid approximation and includes dissipative transport properties such as shear viscosity, bulk viscosity and heat conductivity or baryon diffusion. Keeping for the shear stress, bulk viscous pressure and baryon diffusion current only terms of first order in gradients of the fluid velocity, temperature and chemical potential leads to a covariant version of the well known Navier-Stokes theory, which however, is not an hyperbolic differential equation and can therefore not be used for a time evolution that is causal in the relativistic sense. A way out has been proposed by MÃijller, as well as Israel and Stewart. In their framework, the theoretical setup is modified in such a way that the shear stress, bulk viscous pressure and baryon diffusion current are not related to the gradients of fluid velocity and thermodynamic variables by constraints but rather have their own evolution equation and relax towards the Navier-Stokes values on a proper time scale given by their respective relaxation times. These relaxation times cannot be too small in order to have a causal set of fluid dynamic evolution equations.

It would in fact be great to test the modifications proposed by MÃijller, Israel and Stewart (and subsequent authors) experimentally and to put an experimental bound on the value of the relaxation times (or their ratios to other thermodynamic and transport properties). This would help for a better understanding of relativistic fluid dynamics that is also needed elsewhere, for example in cosmology. However, this is not very easy and can only be done in an interplay of theory and experiment. In fluid dynamic models of heavy ion collisions one can vary the value of second order transport coefficients and study the impact on various flow observables, in particular particle spectra, flow coefficients v_n, flow correlation functions and HBT parameters. By a detailed comparison to experimental data one can put constraints on the second order transport coefficients. A large variety of experimental flow observables, detailed and differential data, as well as small statistical uncertainties are obviously helpful for this endeavor.

3 Initial conditions

As already alluded to in Section 2, the intial state of heavy ion collisions is the major source of uncertainty when it comes to extracting transport properties of the produced medium. This has to do with the fact that calculations of the exact geometry and its fluctuations involve nonperturbative physics. The available descriptions for the initial state thus range from very simplistic models that assign deposited energy densities based on the wounded nucleons or binary collisions determined in a Monte-Carlo Glauber prescription, to classical effective theories of QCD that are valid in the high energy limit. The latter are certainly closer to first principles calculations, and should provide a realistic description of the initial state assuming that the high energy limit is a good approximation.

The major ingredient that needs to be provided by an initial state model is the geometry of the interaction region in the plane transverse to the beam. It is entirely dominated by the positions of incoming nucleons whose fluctuations also play an important role. Observables are also sensitive to the detailed way the energy is deposited given a distribution of wounded nucleons, and the constraints on this from data are surprisingly robust [16]. Using the Trento model it was found that the product of thickness functions of the two nuclei at every given transverse position gives the best description of the data (compared to a conventinal wounded nucleon model or other combinations of thickness functions). This type of energy deposition is very much what the EKRT [29] and IP-Glasma [27, 28] models include, explaining their success in describing a wide range of observables [29, 43].

Fluctuations of wounded nucleon positions contribute the dominant effect to fluctuations of the initial geometry in heavy ion collisions. Smaller scale fluctuations (emerging e.g. from color charge fluctuations in the IP-Glasma model) have been shown to not significantly affect most observables measuring the momentum anoisotropy of produced particles [44]. The factorization breaking ratio shows some sensitivity and it should be pointed out that multiplicity fluctuations are also influenced by the existence of color charge fluctuations.

More recently, indications that the nucleon should possess a substructure of hotspots have emerged. The IP-Glasma model was unable to describe flow coefficients in p+Pb collisions assuming a round proton [45]. Including subnucleonic fluctuations constrained by incoherent diffractive J/ψ production data from HERA [46] (which also require a fluctuating proton geometry) improved the agreement with the p+Pb data significantly [47]. Recent Bayesian analyses also found that nucleon substructure is necessary to simultaneously describe p+Pb and Pb+Pb bulk observables [16]. It should be noted, however, that the size scales for nucleons and subnuclear hot spots extracted in that work are significantly larger than those obtained from comparison to HERA data in the IP-Glasma model.

Initial conditions for hydrodynamic simulations have to provide, in principle, all components of the energy momentum tensor as a function of spatial position (and initial conditions for other conserved charges, if considered). This includes, apart from the always included energy density distribution, the initial flow as well as initial viscous corrections. Initial flow is included in many recently developed models, that either assume free streaming [16], including Yang-Mills evolution, which is close to free streaming [43] or an initial flow distribution motivated by strong coupling calculations [48]. Initial viscous corrections are often set to zero. Only a few works [16, 40, 47] include the full viscous stress tensor provided by the initial state description.

Since the initial state models that provide the entire $T^{\mu\nu}$ all switch from essentially a freely streming system to strongly interacting hydrodynamics at a fixed time τ, that transition is somewhat abrupt and not very physical. To improve over this situation an intermediate step using effective kinetic theory has been introduced [49, 50]. This procedure allows for a somewhat smoother matching but has yet to be used in full fledged hydrodynamic simulations. The effect on observables in heavy ion collisions is likely small, while in small systems, such as p+A a larger effect can be expected.

As already discussed in Section 2, the choice of initial state has a significant effect on the extraction of transport coefficients. A more compact initial state and the presence of initial flow lead to a larger

transverse flow, which requires a larger bulk viscosity to compensate for it and produce agreement with experimental data [40]. Also, the models' eccentricities will affect the final momentum anisotropies, influencing the extracted shear viscosity to entropy density ratio. Two possible attempts to solve this problem have been pursued: Constrain an initial state description as well as possible using data from experiments other than heavy ion collisions (e.g. e+p scattering data, which will hopefully be extended to e+A in a future electron ion collider facility), or perform a combined Bayesian analysis of all parameters, including those of the initial state, to find the best fit for all transport coefficients along with the initial state description.

As mentioned above, at the moment the two approaches lead to some similar features of the initial state (product of thickness functions, presence of subnucleon structure), but also show discrepancies (size of the nucleon and sub-nucleon scales along with the size of the extracted bulk viscosity). Only when the two methods converge for all features of the initial state and medium properties, can one confidently declare that the initial state as well as the transport properties of the QGP are understood.

4 Longitudinal flow fluctuations

- longitudinal flow dynamics studied for first time at LHC
- CMS measurements of EP decorrelation [51]
- ATLAS measurements of magnitude and EP fluctuations [52]
- Currently decorrelation measurements show mostly linear decorrelation with eta, except in most central events.
- Major improvement due to increase of tracking acceptance in run-4 to +-4 units in eta will allow study of non-linear decorrelation.
- possibility of studying longitudinal flow fluctuations via PCA technique [53] done by CMS

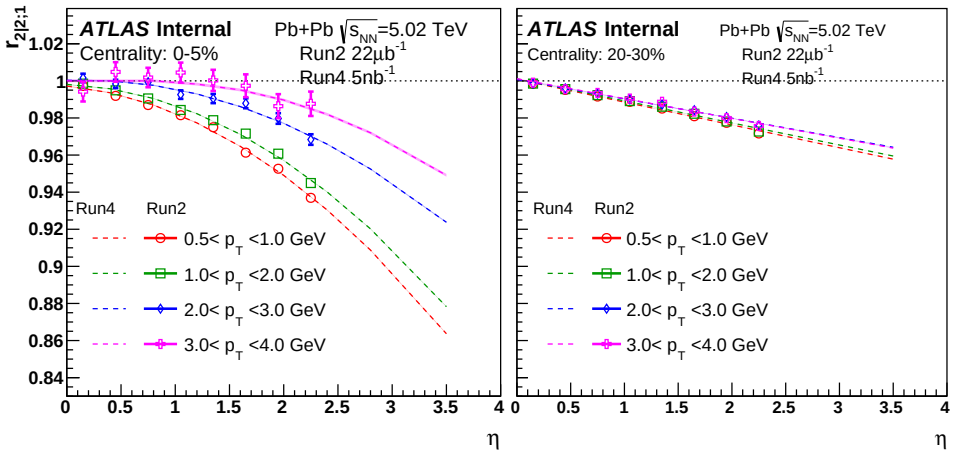

Fig. 1: ATLAS projection plot of longitudinal flow decorrelation in Run-4 due to increased tracking acceptance.

4.1 System size dependence

- Motivation for colliding XeXe, OO, ArAr and other species
- Analysis/measurement of deformation possible
- disentangle geometry and viscous effects
- interpolation points between Pb+Pb, Cu+Cu, p/D/He+A

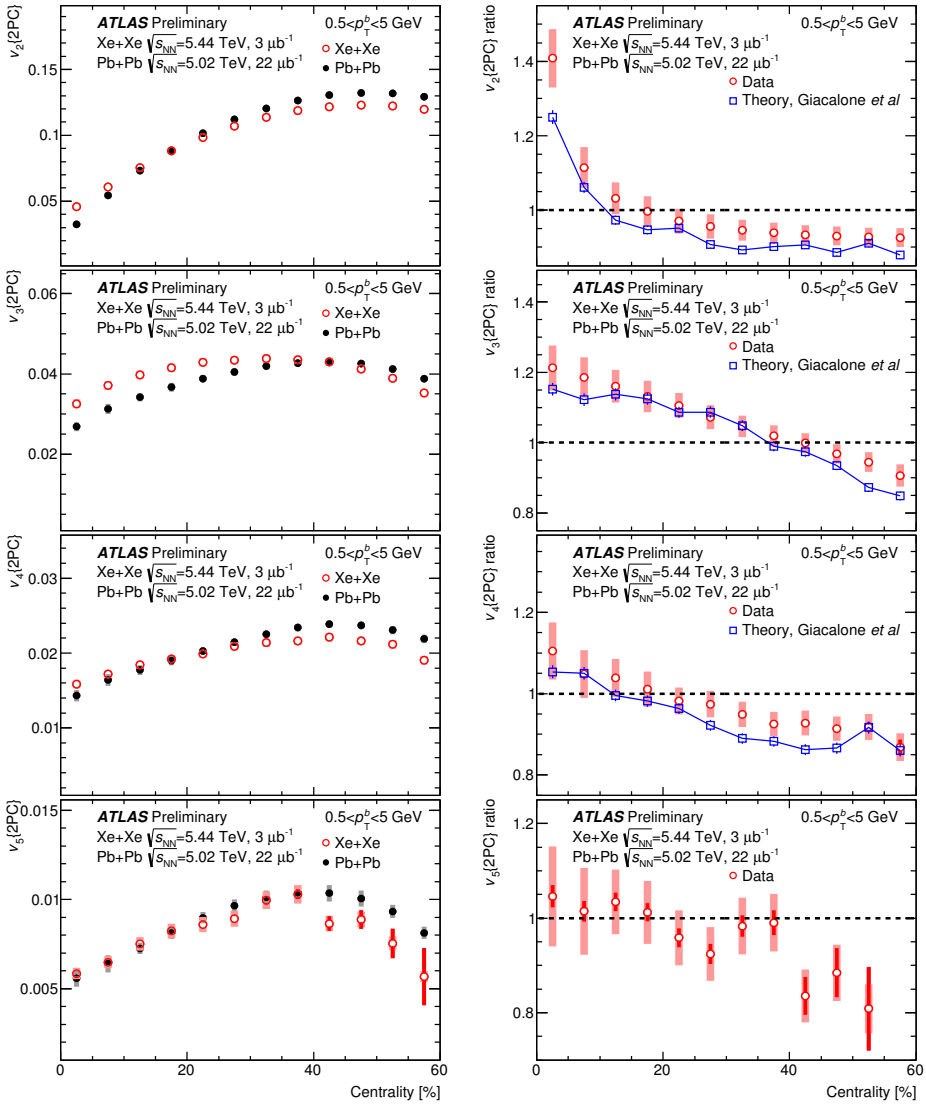

Fig. 2: Figure from Ref. [54]

4.2 Vorticity and polarization

– The estimation for the LHC energy $\sqrt{s_{NN}} = 2.76$ TeV indicate the strength of Abelian magnetic field is $eB \sim 1.0$ GeV^2 very shortly after collisions and it decreases down to the $eB \sim 200$ MeV^2 for time $\tau \sim 0.1$ fm/c without taken into account the electroconductivity of the quark-gluon matter [55–57]. Therefore one can expect $|\Delta P| = 0.61 eB/m_p T \sim (4.3 \pm 0.7) \times 10^{-4}$ for the temperature of the quark-gluon plasma $T = (304 \pm 51)$ MeV [58]. Here m_p is the proton mass, $\Delta P \equiv P_\Lambda - P_{\bar{\Lambda}}$ is the difference in polarization of primary Λ and $\bar{\Lambda}$ [59]. This estimation for $|\Delta P|$ is some smaller than that at RHIC energies due to hotter medium at the LHC. But it should be noted the electroconductivity will lead to noticeably weaker time dependence of the eB [60] and the conductivity may compensate the growth of T and provides the increase of the $|\Delta P|$. Moreover the pass from RHIC to the LHC energy leads to the significant growth of the peak value for eB. Thus for HE–LHC the magnitude of ΔP is expected similar or even larger than at RHIC energies. Furthermore the higher energy of the HE–LHC project provides the novel opportunity for study of polarization of heavier hyperons (for instance, Σ) in hot environment.

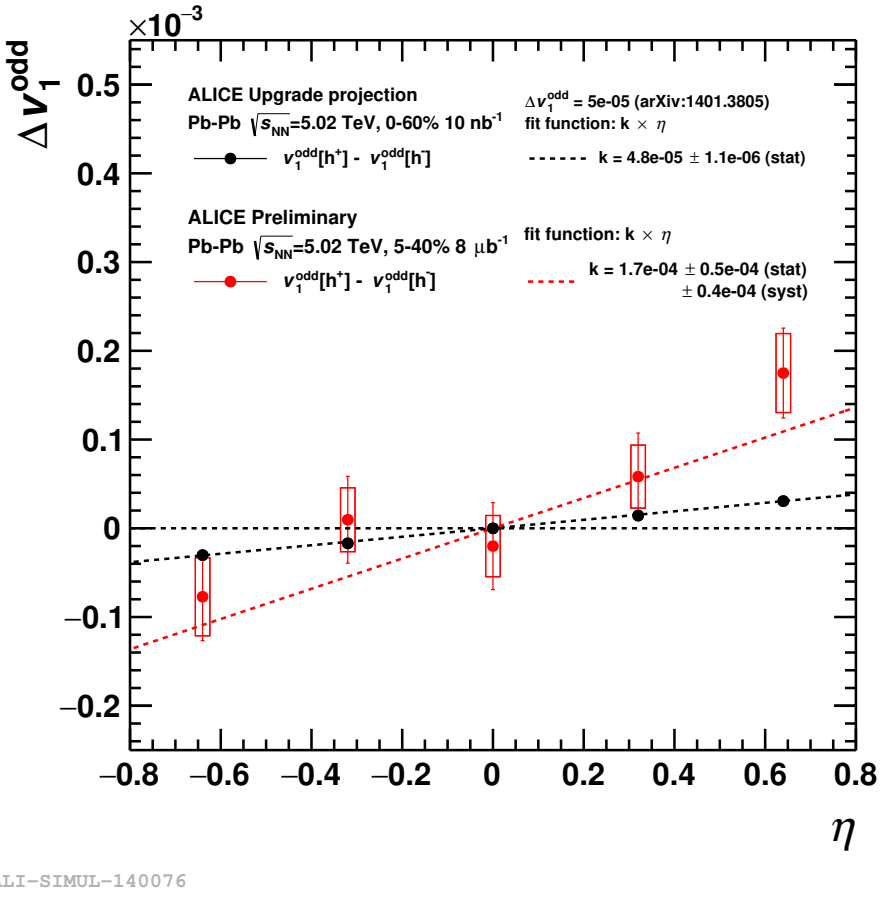

Fig. 3

Fig. 4 presents the energy dependence of the global polarization of Λ and $\bar{\Lambda}$ for the semi-central heavy ion collisions. The RHIC results show the decrease of polarization at higher $\sqrt{s_{NN}}$. But Λ and $\bar{\Lambda}$ demonstrate the finite global polarizations even at highest RHIC energy $\sqrt{s_{NN}} = 200$ GeV [**?**]. The preliminary ALICE data point at $\sqrt{s_{NN}} = 2.76$ TeV is close in magnitude with results at $\sqrt{s_{NN}} = 200$ GeV. But the ALICE upgrade projection at twice large collision energy corresponds to the

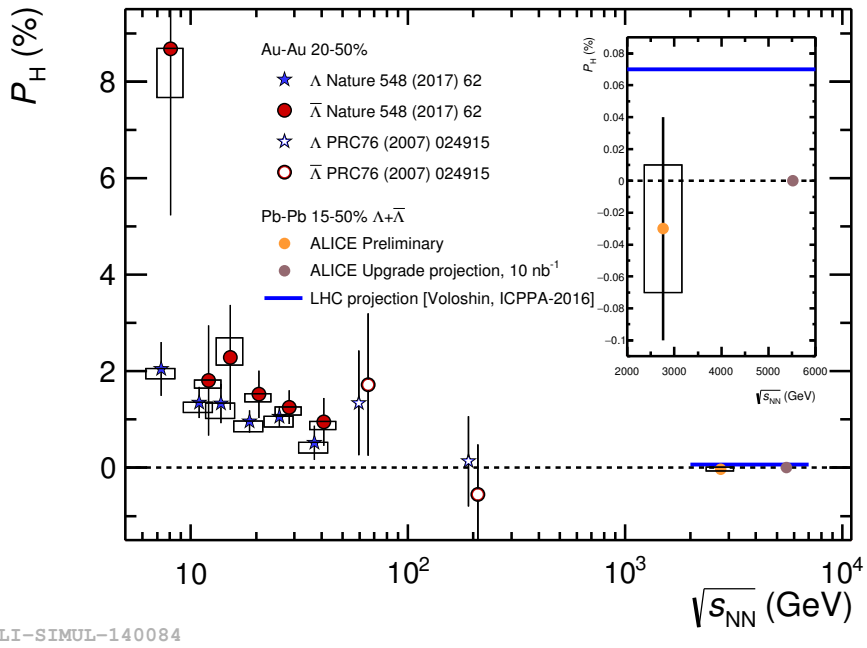

Fig. 4: Global polarization of Λ and $\bar{\Lambda}$ as a function of the collision energy $\sqrt{s_{NN}}$ for semi-central heavy ion collisions. Open boxes and vertical lines show systematic and statistical uncertainties, respectively. Main panel: the data points for $\bar{\Lambda}$ are slightly horizontally shifted for visibility. Inner panel: the LHC energy domain is shown more detailed.

zero polarization with very high precision. Therefore the study of global polarization of Λ and $\bar{\Lambda}$ within HL–LHC project allows the unambiguous conclusion with regard of the values of this physics quantity in TeV-energy domain.

4.3 Chiral effects

– The vacuum of quantum chromodynamics (QCD) is characterized by rich geometry structure which may corresponds to the fractal-like geometry [61].There is a fundamental interrelation between geometry and essential properties of QCD Lagrangian. Structures with non-trivial topology in QCD vacuum are believed to determine the behavior of the $\mathcal{P}/\mathcal{CP}$ fundamental symmetries in the hot quark-gluon matter. Due to higher luminosity at the HL–LHC and / or high multiplicity per event at HE–LHC energy the multiparticle azimuthal correlations can be used for investigations of wide set of chiral effects in strong interaction [**?**], for instance, chiral magnetic effect – CME, chiral magnetic waves – CMW etc. This approach allows the significant suppression of the backgrounds and improvement of reliability of physical conclusions. The study of charge-dependent azimuthal correlations for various types of light flavor particles can be possible with unprecedented precision due to high luminosity of the HL–LHC project. Consequently the quantitative comparison will be allowed for strengths of correlations in meson, baryon–meson and baryon systems. Such measurements will be essential in particular for search for chiral vortical effect – CVE and its study with high precision. Furthermore the higher energies of the HE–LHC project can provide the opportunity for study of flavor dependence of the $\mathcal{P}/\mathcal{CP}$ violation with help the azimuthal correlations for wider set of types of secondary particles including for heavy flavor ones. Thus experimental study of topology of QCD vacuum can be one of the focuses for studies of bulk properties within the HL–LHC, HE–LHC projects.

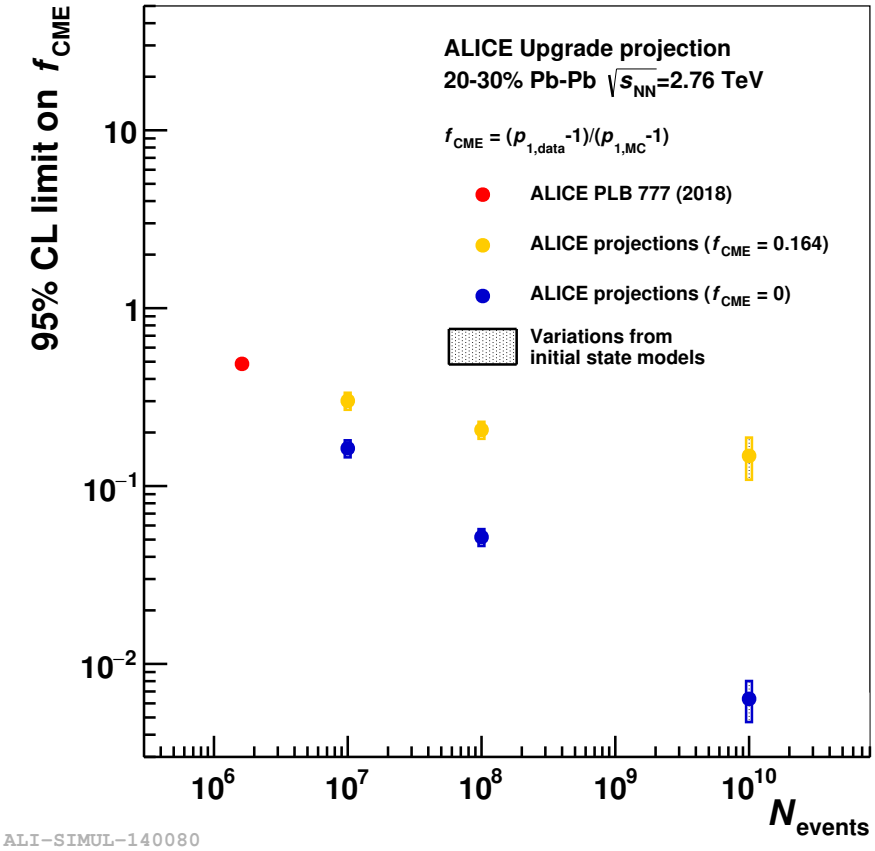

Fig. 5

4.4 Summary

–

References

[1] Y. Aoki, G. Endrodi, Z. Fodor, S. D. Katz, and K. K. Szabo, *The Order of the quantum chromodynamics transition predicted by the standard model of particle physics*, Nature **443** (2006) 675–678, arXiv:hep-lat/0611014 [hep-lat].

[2] P. Steinbrecher, *The QCD crossover at zero and non-zero baryon densities from Lattice QCD*, arXiv:1807.05607 [hep-lat].

[3] O. Kaczmarek, F. Karsch, E. Laermann, C. Miao, S. Mukherjee, P. Petreczky, C. Schmidt, W. Soeldner, and W. Unger, *Phase boundary for the chiral transition in (2+1) -flavor QCD at small values of the chemical potential*, Phys. Rev. **D83** (2011) 014504, arXiv:1011.3130 [hep-lat].

[4] G. Endrodi, Z. Fodor, S. D. Katz, and K. K. Szabo, *The QCD phase diagram at nonzero quark density*, JHEP **04** (2011) 001, arXiv:1102.1356 [hep-lat].

[5] A. Bazavov et al., *Curvature of the freeze-out line in heavy ion collisions*, Phys. Rev. **D93** (2016) no. 1, 014512, arXiv:1509.05786 [hep-lat].

[6] C. Bonati, M. D'Elia, F. Negro, F. Sanfilippo, and K. Zambello, *Curvature of the pseudocritical line in QCD: Taylor expansion matches analytic continuation*, arXiv:1805.02960 [hep-lat].

[7] P. Cea, L. Cosmai, and A. Papa, *Critical line of 2+1 flavor QCD*, Phys. Rev. **D89** (2014) no. 7, 074512, arXiv:1403.0821 [hep-lat].

[8] C. Bonati, P. de Forcrand, M. D'Elia, O. Philipsen, and F. Sanfilippo, *Chiral phase transition in two-flavor QCD from an imaginary chemical potential*, Phys. Rev. **D90** (2014) no. 7, 074030, arXiv:1408.5086 [hep-lat].

[9] C. Bonati, M. D'Elia, M. Mariti, M. Mesiti, F. Negro, and F. Sanfilippo, *Curvature of the chiral pseudocritical line in QCD: Continuum extrapolated results*, Phys. Rev. **D92** (2015) no. 5, 054503, arXiv:1507.03571 [hep-lat].

[10] R. Bellwied, S. Borsanyi, Z. Fodor, J. GÃijnther, S. D. Katz, C. Ratti, and K. K. Szabo, *The QCD phase diagram from analytic continuation*, Phys. Lett. **B751** (2015) 559–564, arXiv:1507.07510 [hep-lat].

[11] P. Cea, L. Cosmai, and A. Papa, *Critical line of 2+1 flavor QCD: Toward the continuum limit*, Phys. Rev. **D93** (2016) no. 1, 014507, arXiv:1508.07599 [hep-lat].

[12] P. Huovinen and P. Petreczky, *QCD Equation of State and Hadron Resonance Gas*, Nucl. Phys. **A837** (2010) 26–53, arXiv:0912.2541 [hep-ph].

[13] S. Borsanyi, Z. Fodor, C. Hoelbling, S. D. Katz, S. Krieg, and K. K. Szabo, *Full result for the QCD equation of state with 2+1 flavors*, Phys. Lett. **B730** (2014) 99–104, arXiv:1309.5258 [hep-lat].

[14] HotQCD Collaboration, A. Bazavov et al., *Equation of state in (2+1)-flavor QCD*, Phys. Rev. D **90** (2014) 094503, arXiv:1407.6387 [hep-lat].

[15] J. S. Moreland and R. A. Soltz, *Hydrodynamic simulations of relativistic heavy-ion collisions with different lattice quantum chromodynamics calculations of the equation of state*, Phys. Rev. **C93** (2016) no. 4, 044913, arXiv:1512.02189 [nucl-th].

[16] J. S. Moreland, J. E. Bernhard, and S. A. Bass, *Estimating initial state and quark-gluon plasma medium properties using a hybrid model with nucleon substructure calibrated to p-Pb and Pb-Pb collisions at* $\sqrt{s_{\rm NN}} = 5.02$ *TeV*, arXiv:1808.02106 [nucl-th].

[17] P. F. Kolb and U. W. Heinz, *Hydrodynamic description of ultrarelativistic heavy ion collisions*, arXiv:nucl-th/0305084 [nucl-th].

[18] P. Huovinen, *Hydrodynamical description of collective flow. Chapter 1.*, arXiv:nucl-th/0305064 [nucl-th].

[19] T. Hirano and K. Tsuda, *Collective flow and two pion correlations from a relativistic*

hydrodynamic model with early chemical freezeout, Phys. Rev. **C66** (2002) 054905, arXiv:nucl-th/0205043 [nucl-th].

[20] P. B. Arnold, G. D. Moore, and L. G. Yaffe, *Transport coefficients in high temperature gauge theories. 2. Beyond leading log*, JHEP **05** (2003) 051, arXiv:hep-ph/0302165 [hep-ph].

[21] J. Ghiglieri, G. D. Moore, and D. Teaney, *Second-order Hydrodynamics in Next-to-Leading-Order QCD*, Phys. Rev. Lett. **121** (2018) no. 5, 052302, arXiv:1805.02663 [hep-ph].

[22] A. Nakamura and S. Sakai, *Transport coefficients of gluon plasma*, Phys. Rev. Lett. **94** (2005) 072305, arXiv:hep-lat/0406009 [hep-lat].

[23] H. B. Meyer, *A Calculation of the shear viscosity in SU(3) gluodynamics*, Phys. Rev. **D76** (2007) 101701, arXiv:0704.1801 [hep-lat].

[24] S. BorsÃąnyi, Z. Fodor, M. Giordano, S. D. Katz, A. Pasztor, C. Ratti, A. SchÃd'fer, K. K. Szabo, and B. TÃşth, *High statistics lattice study of stress tensor correlators in pure $SU(3)$ gauge theory*, Phys. Rev. **D98** (2018) no. 1, 014512, arXiv:1802.07718 [hep-lat].

[25] C. Gale, S. Jeon, and B. Schenke, *Hydrodynamic Modeling of Heavy-Ion Collisions*, Int. J. Mod. Phys. **A28** (2013) 1340011, arXiv:1301.5893 [nucl-th].

[26] U. Heinz and R. Snellings, *Collective flow and viscosity in relativistic heavy-ion collisions*, Ann. Rev. Nucl. Part. Sci. **63** (2013) 123–151, arXiv:1301.2826 [nucl-th].

[27] B. Schenke, P. Tribedy, and R. Venugopalan, *Fluctuating Glasma initial conditions and flow in heavy ion collisions*, Phys. Rev. Lett. **108** (2012) 252301, arXiv:1202.6646 [nucl-th].

[28] B. Schenke, P. Tribedy, and R. Venugopalan, *Event-by-event gluon multiplicity, energy density, and eccentricities in ultrarelativistic heavy-ion collisions*, Phys. Rev. **C86** (2012) 034908, arXiv:1206.6805 [hep-ph].

[29] H. Niemi, K. J. Eskola, and R. Paatelainen, *Event-by-event fluctuations in a perturbative QCD + saturation + hydrodynamics model: Determining QCD matter shear viscosity in ultrarelativistic heavy-ion collisions*, Phys. Rev. **C93** (2016) no. 2, 024907, arXiv:1505.02677 [hep-ph].

[30] S. Ryu, J.-F. Paquet, C. Shen, G. Denicol, B. Schenke, S. Jeon, and C. Gale, *Effects of bulk viscosity and hadronic rescattering in heavy ion collisions at energies available at the BNL Relativistic Heavy Ion Collider and at the CERN Large Hadron Collider*, Phys. Rev. **C97** (2018) no. 3, 034910, arXiv:1704.04216 [nucl-th].

[31] A. Buchel, *Bulk viscosity of gauge theory plasma at strong coupling*, Phys. Lett. **B663** (2008) 286–289, arXiv:0708.3459 [hep-th].

[32] S. I. Finazzo, R. Rougemont, H. Marrochio, and J. Noronha, *Hydrodynamic transport coefficients for the non-conformal quark-gluon plasma from holography*, JHEP **02** (2015) 051, arXiv:1412.2968 [hep-ph].

[33] R. Horsley and W. Schoenmaker, *Quantum Field Theories Out of Thermal Equilibrium. 1. General Considerations*, Nucl. Phys. **B280** (1987) 716–734.

[34] P. B. Arnold, C. Dogan, and G. D. Moore, *The Bulk Viscosity of High-Temperature QCD*, Phys. Rev. **D74** (2006) 085021, arXiv:hep-ph/0608012 [hep-ph].

[35] F. Karsch, D. Kharzeev, and K. Tuchin, *Universal properties of bulk viscosity near the QCD phase transition*, Phys. Lett. **B663** (2008) 217–221, arXiv:0711.0914 [hep-ph].

[36] H. B. Meyer, *A Calculation of the bulk viscosity in SU(3) gluodynamics*, Phys. Rev. Lett. **100** (2008) 162001, arXiv:0710.3717 [hep-lat].

[37] D. Kharzeev and K. Tuchin, *Bulk viscosity of QCD matter near the critical temperature*, JHEP **09** (2008) 093, arXiv:0705.4280 [hep-ph].

[38] G. S. Denicol, T. Kodama, T. Koide, and P. Mota, *Effect of bulk viscosity on Elliptic Flow near QCD phase transition*, Phys. Rev. **C80** (2009) 064901, arXiv:0903.3595 [hep-ph].

[39] J. Noronha-Hostler, J. Noronha, and C. Greiner, *Transport Coefficients of Hadronic Matter near*

T(c), Phys. Rev. Lett. **103** (2009) 172302, arXiv:0811.1571 [nucl-th].

[40] B. Schenke, C. Shen, and P. Tribedy, *Features of the IP-Glasma*, in *27th International Conference on Ultrarelativistic Nucleus-Nucleus Collisions (Quark Matter 2018) Venice, Italy, May 14-19, 2018*. 2018. arXiv:1807.05205 [nucl-th].

[41] P. Bozek, *Bulk and shear viscosities of matter created in relativistic heavy-ion collisions*, Phys. Rev. **C81** (2010) 034909, arXiv:0911.2397 [nucl-th].

[42] J.-F. Paquet, C. Shen, G. S. Denicol, M. Luzum, B. Schenke, S. Jeon, and C. Gale, *Production of photons in relativistic heavy-ion collisions*, Phys. Rev. **C93** (2016) no. 4, 044906, arXiv:1509.06738 [hep-ph].

[43] C. Gale, S. Jeon, B. Schenke, P. Tribedy, and R. Venugopalan, *Event-by-event anisotropic flow in heavy-ion collisions from combined Yang-Mills and viscous fluid dynamics*, Phys. Rev. Lett. **110** (2013) no. 1, 012302, arXiv:1209.6330 [nucl-th].

[44] F. G. Gardim, F. Grassi, P. Ishida, M. Luzum, P. S. MagalhÃčes, and J. Noronha-Hostler, *Sensitivity of observables to coarse-graining size in heavy-ion collisions*, Phys. Rev. **C97** (2018) no. 6, 064919, arXiv:1712.03912 [nucl-th].

[45] B. Schenke and R. Venugopalan, *Eccentric protons? Sensitivity of flow to system size and shape in p+p, p+Pb and Pb+Pb collisions*, Phys. Rev. Lett. **113** (2014) 102301, arXiv:1405.3605 [nucl-th].

[46] H. MÃd'ntysaari and B. Schenke, *Evidence of strong proton shape fluctuations from incoherent diffraction*, Phys. Rev. Lett. **117** (2016) no. 5, 052301, arXiv:1603.04349 [hep-ph].

[47] H. MÃd'ntysaari, B. Schenke, C. Shen, and P. Tribedy, *Imprints of fluctuating proton shapes on flow in proton-lead collisions at the LHC*, Phys. Lett. **B772** (2017) 681–686, arXiv:1705.03177 [nucl-th].

[48] R. D. Weller and P. Romatschke, *One fluid to rule them all: viscous hydrodynamic description of event-by-event central p+p, p+Pb and Pb+Pb collisions at* $\sqrt{s} = 5.02$ *TeV*, Phys. Lett. **B774** (2017) 351–356, arXiv:1701.07145 [nucl-th].

[49] A. Kurkela, A. Mazeliauskas, J.-F. Paquet, S. Schlichting, and D. Teaney, *Matching the non-equilibrium initial stage of heavy ion collisions to hydrodynamics with QCD kinetic theory*, arXiv:1805.01604 [hep-ph].

[50] A. Kurkela, A. Mazeliauskas, J.-F. Paquet, S. Schlichting, and D. Teaney, *Effective kinetic description of event-by-event pre-equilibrium dynamics in high-energy heavy-ion collisions*, arXiv:1805.00961 [hep-ph].

[51] CMS Collaboration, *Pseudorapidity and transverse momentum dependence of flow harmonics in pPb and PbPb collisions*, arXiv:1710.07864 [hep-ex].

[52] ATLAS Collaboration, *Measurement of longitudinal flow de-correlations in Pb+Pb collisions at* $\sqrt{s_{\rm NN}} = 2.76$ *and 5.02 TeV with the ATLAS detector*, arXiv:1709.02301 [hep-ex].

[53] R. S. Bhalerao, J.-Y. Ollitrault, S. Pal, and D. Teaney, *Principal component analysis of event-by-event fluctuations*, Phys. Rev. Lett. **114** (2015) no. 15, 152301, arXiv:1410.7739 [nucl-th].

[54] ATLAS Collaboration, *Measurement of the azimuthal anisotropy of charged particle production in Xe+Xe collisions at* $\sqrt{s_{\rm NN}}$*=5.44 TeV with the ATLAS detector*, ATLAS-CONF-2018-011, CERN, Geneva, May, 2018. https://cds.cern.ch/record/2318870.

[55] Y. Zhong, C.-B. Yang, X. Cai, and S.-Q. Feng, *A systematic study of magnetic field in relativistic heavy-ion collisions in the RHIC and LHC energy regions*, Adv. High Energy Phys. **2014** (2014) 193039, arXiv:1408.5694 [hep-ph].

[56] V. Okorokov and P. Parfenov, *Particle correlators and possible local parity violation in nuclear collisions*, J. Phys. Conf. Ser. **668** (2016) 012129.

[57] V. Okorokov and P. Parfenov, *Charge-dependent azimuthal correlations of secondary particles in heavy ion collisions*, J. Phys. Conf. Ser. **675** (2016) 022021.

[58] M. Wilde, *Measurement of direct photons in pp and Pb-Pb collisions with ALICE*, Nucl. Phys. A **904-905** (2013) 573c, arXiv:1210.5958 [hep-ex].

[59] F. Becattini, I. Karpenko, M. A. Lisa, I. Upsal, and S. A. Voloshin, *Global hyperon polarization at local thermodynamic equilibrium with vorticity, magnetic field, and feed-down*, Phys. Rev. C **95** (2017) no. 5, 054902, arXiv:1610.02506 [nucl-th].

[60] K. Tuchin, *Particle production in strong electromagnetic fields in relativistic heavy-ion collisions*, Adv. High Energy Phys. **2013** (2013) 490495, arXiv:1301.0099 [hep-ph].

[61] V. Okorokov, *Dependence of asymmetries for charge distribution with respect to the reaction plane on initial energy in heavy-ion collisions*, Int. J. Mod. Phys. E **22** (2013) no. 6, 1350041, arXiv:1301.0880 [nucl-ex].